ELSEVIER SAUNDERS

RADIOLOGIC CLINICS OF NORTH AMERICA

Radiol Clin N Am 44 (2006) 503–523

MR Imaging of the Rotator Cuff

Ara Kassarjian, MD, FRCPC[a,*], Jenny T. Bencardino, MD[b], William E. Palmer, MD[a]

Repetitive overhead motions, such as those commonly employed in tennis, baseball, swimming, and football, can lead to primary rotator cuff impingement [1]. Primary impingement is often seen in middle-aged athletes who present with chronic pain and weakness associated with overhead sporting activities. Conversely, secondary impingement is typically a manifestation of glenohumeral instability and is more common in young athletes who employ overhead or throwing motions. Although less common, secondary impingement may also be seen in the setting of posterior superior impingement and scapulothoracic instability. Prompt and accurate diagnosis of impingement syndromes helps ensure timely and appropriate treatment of recreational and professional athletes.

MR imaging is an accurate method of evaluating the rotator cuff, coracoacromial arch, and the subacromial-subdeltoid bursa [2,3]. In addition, MR imaging can often identify lesions responsible for instability and secondary impingement. This article addresses the role of MR imaging in evaluating the rotator cuff and the importance of MR imaging in identifying other lesions that may mimic rotator cuff pathology. A rationale for protocol design, including MR arthrography and the use of specialized positioning, such as abduction and external rotation (ABER), are discussed.

MR imaging protocol

Although there are innumerable ways of performing MR imaging of the shoulder, a few fundamental principles should be applied. Use of a local surface coil, such as a dedicated phased array coil, is mandatory to ensure adequate spatial resolution and signal to noise and thereby achieve high-quality imaging. The patient is typically in the supine position with the arm slightly externally rotated at their side. To ensure mild external rotation, we place a rolled towel under the elbow, which typically results in a comfortable slightly externally rotated position, thereby reducing motion artifact resulting from patient discomfort.

This article was previously published in *Magnetic Resonance Imaging Clinics of North America* 2004;12:39–60.
[a] Musculoskeletal MRI, Massachusetts General Hospital, 15 Parkman Street, Suite 515, Boston, MA 02114, USA
[b] Musculoskeletal Radiology, Medical Arts Radiology Group, PC, Huntington Hospital, North Shore-Long Island Jewish Hospital Health System, 270 Park Avenue, Huntington, NY 11743, USA
* Corresponding author.
E-mail address: akassarjian@partners.org (A. Kassarjian).

0033-8389/06/$ – see front matter
doi:10.1016/j.rcl.2006.04.005
radiologic.theclinics.com

Our current protocol includes coronal oblique, sagittal oblique, and axial imaging planes. Axial proton density (2500/20) or gradient echo (550/15, flip angle 20) images should extend from the top of the acromioclavicular joint though the inferior glenoid margin. Coronal oblique proton density (2500/20), fast spin-echo T2-weighted (3800/100, ETL 8), and fast spin-echo intermediate TE (2700/50, ETL 6) fat-suppressed images are prescribed perpendicular to the glenoid cavity. Alternatively, these can be prescribed parallel to the supraspinatus tendon. The oblique coronal images extend form the subscapularis anteriorly to the infraspinatus and teres minor posteriorly. Oblique sagittal images are oriented perpendicular to the oblique coronal images (ie, parallel to the glenoid cavity). T1-weighted and fast-inversion recovery or fat-suppressed T2-weighted images in the oblique sagittal plane extend from the body of the scapula through the greater tuberosity. It is critical to ensure that the most lateral image covers the distal fibers of the supraspinatus and infraspinatus as they insert on the greater tuberosity. Although this protocol produces excellent imaging of the rotator cuff, partial-thickness undersurface tears and small full-thickness tears may not be visible in the absence of an effusion because of insufficient signal differences between the rotator cuff and the adjacent humeral head.

MR arthrography exploits the advantages gained from the presence of a joint effusion. Dilution of commercially available gadolinium formulations to a concentration of approximately 2 mmol ensures optimization of paramagnetic effects on T1-weighted imaging. To obtain this concentration, 0.4 mL of gadopentate dimeglumine (Magnevist, Berlex Laboratories, Wayne, New Jersey) are added to 50 cc of normal saline. Ten milliliters of this solution are mixed with 5 mL of nonionic iodinated contrast and 5 mL of preservative free lidocaine 1%, resulting in a final gadolinium dilution of 1:250. A 22-gauge 3.5-in spinal needle is advanced into the glenohumeral joint under fluoroscopic guidance, and 12 to 15 mL of this solution is injected to achieve adequate capsular distention. The addition of iodinated contrasted into the solution allows for fluoroscopic confirmation of intra-articular injection. Also, standard pre- and postexercise fluoroscopic images can be obtained. MR imaging is initiated within 30 minutes of injection to avoid loss of capsular distention as the fluid is absorbed out of the joint. Some institutions add a small quantity of epinephrine to the solution to achieve vasoconstriction and thus delay resorption of the contrast from the glenohumeral joint. This technique may be beneficial if there is a potential for delay between injection and initiation of MR scanning.

The MR arthrographic protocol takes advantage of the T1 shortening effects of gadolinium. We employ routine three-plane spin-echo frequency selective fat-suppressed T1-weighted sequences, a coronal oblique fast spin-echo T2-weighted sequence, and a sagittal oblique spin-echo T1-weighted sequence. For younger patients and patients suspected of having posterior superior impingement and partial-thickness undersurface tears, the arm is placed in the abduction and external rotation (ABER) position with the patient's palm under the head. Oblique axial fat-suppressed T1-weighted images of the glenohumeral joint are then obtained. The ABER position is valuable in demonstrating lesions of posterior superior impingement and undersurface tears of the rotator cuff as well as nondisplaced tears of the anterior inferior labrum in patients with glenohumeral instability [4].

Anatomic considerations

The tendons of the supraspinatus, infraspinatus, subscapularis, and teres minor comprise the rotator cuff. The subscapularis inserts on the lesser tuberosity, with superficial fibers extending to the greater tuberosity and thus contributing to the transverse humeral ligament, which forms the roof of the intertubercular (bicipital) groove. The supraspinatus, infraspinatus, and teres minor insert onto the superior, middle, and inferior facets of the greater tuberosity, respectively. The rotator interval is a triangular-shaped space between the anterior fibers of the supraspinatus and the superior fibers of the subscapularis. The coracoid process forms the base of this space, and the transverse humeral ligament forms the apex. The coracohumeral ligament, the superior glenohumeral ligament, and the tendon of the long head biceps brachii are intimately related to the rotator interval (Fig. 1). All four muscles of the rotator cuff act as stabilizers of the glenohumeral joint. The supraspinatus is primarily a shoulder abductor. The infraspinatus and teres minor externally rotate the shoulder, with the former also being an abductor and the latter being a weak adductor. The subscapularis is a strong adductor and internal rotator [5,6].

The supraspinatus muscle originates along the dorsal surface of the scapula within the supraspinous fossa. The muscle fibers course along a lateral orientation and converge to form a dominant single tendon along the anterior aspect of the muscle. The myotendinous junction is typically at the 12 o'clock position above the humeral head, although there is some slight variation in this position (Fig. 2) (see later discussion) [7]. The supraspinatus tendon is bordered superiorly by the subacromial-subdeltoid

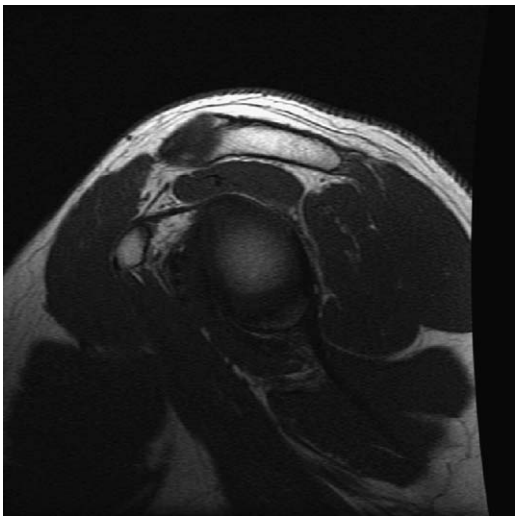

Fig. 1. Rotator interval. Sagittal oblique T1-weighted image shows normal rotator interval between the supraspinatus and the subscapularis.

bursa and inferiorly by the joint capsule. Anteriorly, the more distal supraspinatus tendon converges with the coracohumeral ligament, and posteriorly it merges with the anterior fibers of the infraspinatus tendon. The supraspinatus tendon is best evaluated in the coronal oblique plane and the sagittal oblique plane, with the latter being helpful in evaluating the most anterior fibers of the supraspinatus. The region just medial to the convergence of the posterior fibers of the supraspinatus and the anterior fibers of the infraspinatus has been referred to as the posterior rotator interval. The supraspinatus is innervated by the suprascapular nerve (C5 and C6), which passes through the suprascapular notch and courses obliquely and laterally along the undersurface of the supraspinatus [8].

The infraspinatus originates in the infraspinous fossa. As opposed to the supraspinatus, which converges to a single dominant tendon, the infraspinatus has a multipennate configuration with the myotendinous junction having a somewhat fanlike configuration (Fig. 3). The infraspinatus is separated from the overlying deltoid by a fascial layer. The inferior margin of the infraspinatus blends with the joint capsule. The distal fibers of the suprascapular nerve, once they pass through a fibro-osseous tunnel at the spinoglenoid notch, innervate the infraspinatus muscle. These distal nerve fibers of the suprascapular nerve terminate within the infraspinatus. The infraspinatus is best evaluated in the coronal oblique and sagittal oblique planes. The teres minor originates along the upper two thirds of the lateral border of the scapula and blends into the posterior glenohumeral joint capsule more distally (see Fig. 3).

The teres minor forms the superior border of the quadrilateral space and the triangular space (Fig. 4). The quadrilateral space is bordered by the teres minor superiorly, the teres major inferiorly, the long head triceps medially, and the surgical neck of the humerus laterally. The quadrilateral space contains the axillary nerve and the posterior circumflex vessels. The triangular space is more medially located and is bordered by the teres minor superomedially, the teres major inferomedially, and the long head triceps laterally. The triangular space contains the circumflex scapular artery. Although the quadrilateral space and triangular space

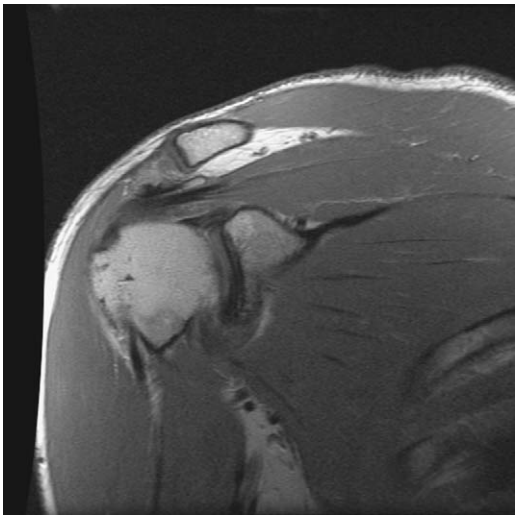

Fig. 2. Supraspinatus. Coronal oblique proton density image shows normal supraspinatus myotendinous junction.

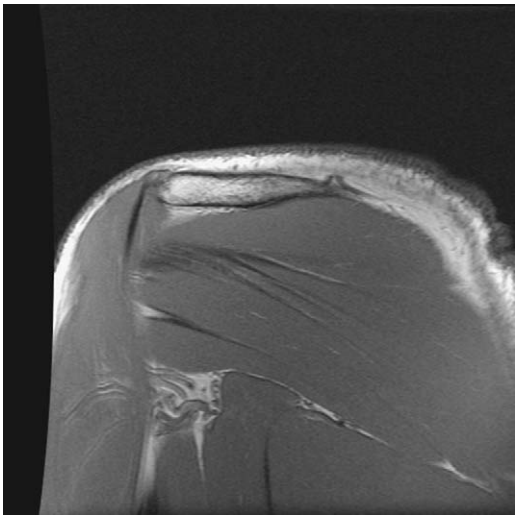

Fig. 3. Infraspinatus and teres minor. Coronal oblique proton density image shows normal infraspinatus and teres minor.

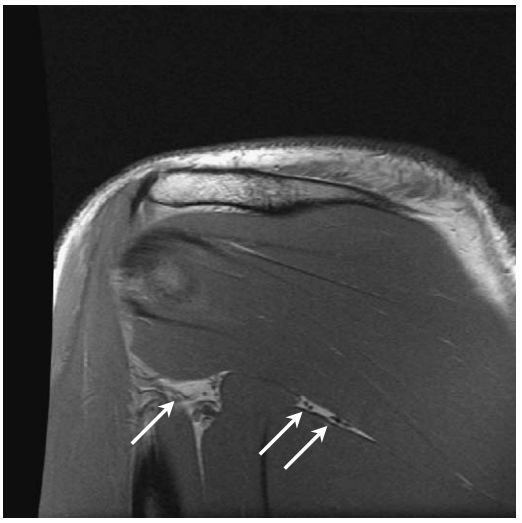

Fig. 4. Quadrilateral space and triangular space. Coronal oblique proton density image shows normal quadrilateral space (*arrow*) and triangular space (*double arrow*).

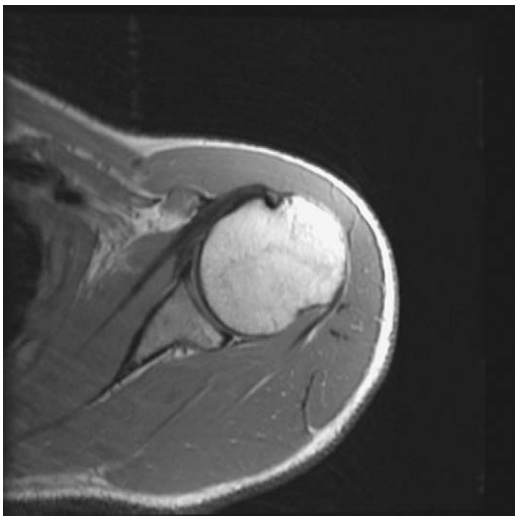

Fig. 5. Subscapularis. Axial oblique image shows normal subscapularis tendon.

are clearly delineated in the coronal oblique plane, the teres minor muscle is best evaluated in the axial and sagittal oblique planes.

The subscapularis muscle originates from the subscapular fossa along the anterior aspect of the scapula. Similar to the infraspinatus, the subscapularis has a multipennate configuration. The subscapularis recess, which communicates with the glenohumeral joint, separates the subscapularis muscle from the coracoid. The deep fibers of the subscapularis tendon blend with and reinforce the anterior capsule of the glenohumeral joint (Fig. 5). The mid and distal portions of the middle glenohumeral ligament blend with the capsule and deep fibers of the subscapularis before inserting into the lesser tuberosity [9]. The subscapularis is best evaluated in the axial and sagittal oblique planes.

The coracoacromial arch is composed of the undersurface of the acromion, the anterior portion of the coracoid, the coracoacromial ligament, the distal clavicle, and the undersurface of the acromioclavicular joint (Fig. 6). The supraspinatus, infraspinatus, long head biceps, and subacromial bursa pass under the coracoacromial arch. The coracoacromial arch is best evaluated in the sagittal oblique and coronal oblique planes.

Rotator cuff impingement

Rotator cuff impingement can take various forms, and attempts have been made to classify impingement syndromes. The following is only one of several methods of classifying rotator cuff impingement.

Primary extrinsic impingement includes subacromial and subcoracoid impingement. Subacromial impingement refers to impingement of the rotator cuff, typically the supraspinatus, as it passes under the coracoacromial arch. Potential etiologies of subacromial impingement include subacromial spurs, variations in acromial morphology or position, hypertrophic acromioclavicular joint abnormalities, an unstable os acromiale, subacromial-subdeltoid bursitis, and thickening of the coracoacromial ligament [10]. Subcoracoid impingement is associated with abnormalities of the coracoid process that result in a decrease in the distance between the coracoid and the anterior aspect of the humeral head.

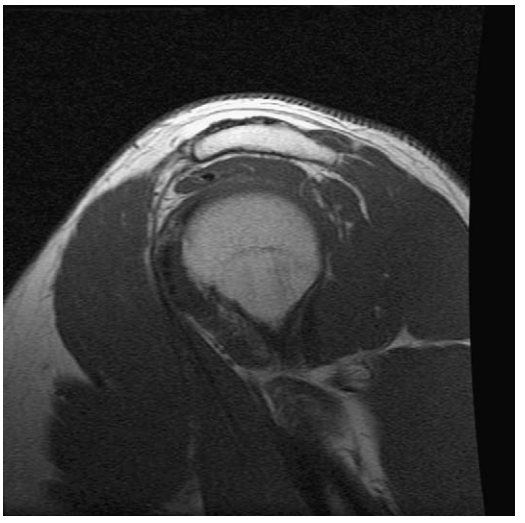

Fig. 6. Coracoacromial arch. Sagittal oblique T1-weighted image shows normal coracoacromial arch.

This abnormal relationship typically results in impingement of the subscapularis and the long head biceps brachii [11,12].

Secondary extrinsic impingement occurs in the setting of a normal coracoacromial arch [13]. In this setting, impingement results from abnormal glenohumeral or scapulothoracic motion secondary to instability.

Internal impingement refers to contact between the glenoid rim and the undersurface of the rotator cuff, particularly when the arm is in the late cocking phase of a throwing motion with the arm in 90 degrees of abduction and maximal external rotation [14]. Internal impingement also may result from narrowing of the coracoacromial outlet as a result of supraspinatus hypertrophy or abnormalities of the greater tuberosity [10].

Primary extrinsic impingement: subacromial

Subacromial impingement refers to a clinical syndrome in which the subacromial bursa and supraspinatus are entrapped underneath the coracoacromial arch. The etiology of this syndrome is variable, including subacromial spurs, undersurface acromioclavicular joint osteophytes, morphologic variations of the acromion, such as anterior down sloping, lateral down sloping, or low-lying acromion, an os acromiale, or a thickened coracoacromial ligament [3]. These anatomic abnormalities lead to a decrease in the space beneath the coracoacromial arch. As this space is reduced, repeated microtrauma to the subacromial bursa and supraspinatus tendon is thought to lead to bursitis and tendon injury. Although the anatomic abnormalities may be identified on MR imaging, they should only be considered a substrate for impingement as the diagnosis of impingement is based on clinical criteria. Provocative tests, such as full forward flexion and internal rotation (Neer's sign) or internal rotation of a 90-degree flexed arm (Hawkins' sign), which result in pain are considered positive clinical signs of subacromial impingement [15]. The former is thought to compress the greater tuberosity against the anterior acromion, whereas the latter is thought to compress the greater tuberosity against the leading edge of the coracoacromial ligament. Occasionally, a diagnostic injection of lidocaine within the subacromial region is employed to help differentiate an impingement syndrome from other etiologies of shoulder pain. If such a diagnostic injection has been performed, MR imaging should be delayed for at least 24 hours to avoid misinterpretation of subacromial fluid as evidence of bursitis or rotator cuff tear [16].

Although MR imaging provides excellent anatomic detail of the components of the rotator cuff and the coracoacromial arch, the patient is typically scanned with the arm at their side, a position that does not reflect the physiologic position of impingement [17]. Despite this limitation, MR imaging is useful in demonstrating potential substrates for impingement involving the coracoacromial arch and supraspinatus outlet. The supraspinatus, superior (anterior) 20% of the infraspinatus, and the subscapularis pass through the coracoacromial arch before their insertion onto the humerus [6].

The sagittal oblique plane is the optimal plane for evaluation of the coracoacromial ligament. The coracoacromial ligament, which has somewhat trapezoidal shape, extends from the coracoid to the undersurface of the acromion. The thickness of the coracoacromial ligament varies from 2 to 5.6 mm [18]. It may be difficult to distinguish a thickened acromial insertion of the coracoacromial ligament from an unossified subacromial spur as both may have low signal intensity on MR imaging. In addition, the deltoid ligament, which has an origin on the acromion along its inferomedial margin, may also be misinterpreted as a subacromial spur (see Fig. 6) [19]. Given these potential pitfalls, unless there is an ossified subacromial spur with intrinsic marrow signal, one must be cautious in ascribing subacromial low signal intensity to a subacromial spur (Fig. 7). Although a subacromial spur is thought to be a cause for subacromial impingement, it is not entirely clear whether coracoacromial ligament degeneration and subacromial spur formation are substrates for impingement or whether they represent sequelae of supraspinatus tendon degeneration [20,21].

Although not universally accepted, variations in the configuration of the acromion have been implicated in the pathogenesis of impingement

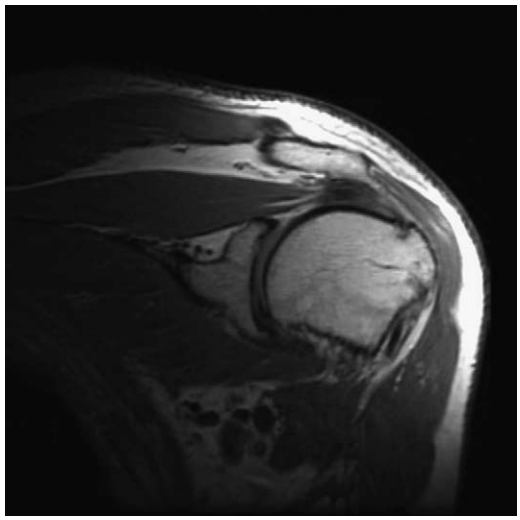

Fig. 7. Subacromial spur. Coronal oblique proton density image shows subacromial spur.

syndromes. Bigliani et al [22] described three acromial configurations. A type I acromion has a flat undersurface and is not thought to be implicated in subacromial impingement. A type II acromion has a concave undersurface and may have a moderate association with subacromial impingement. A type III acromion has a hooked anterior margin (Fig. 8). In a recent study of acromial morphology, type II was the most common (63%), and type III was the least common (14%) [23]. Some researchers believe that acromial morphology is developmental, as evidenced in one study by the lack of association between age, acromial type, and symmetry of acromial shape [24]. Type II and III acromia appear to be more strongly associated with subacromial spur formation. Thus, based on Neer's theory of impingement, which is not universally accepted, individuals with type II and III acromia should be at increased risk for rotator cuff pathology. In support of this theory, two studies demonstrated that 70% to 80% of cuff tears were associated with type III acromia [25,26]. Alternatively, some feel that subacromial spurs are a consequence of, and not a cause for, rotator cuff pathology [20,21]. As opposed to Neer's theory of impingement resulting in cuff abnormalities, some investigators feel that bursal surface cuff abnormalities result in subacromial spur formation. Along the same lines, some feel that the type III acromion is not truly a developmental configuration but actually represents an acquired enthesophyte or calcification/ossification at the coracoacromial attachment onto the anterior acromion [27,28]. Despite disagreement regarding pathogenesis of acromial morphology, oblique sagittal MR images clearly demonstrate the shape of the acromion. However, there may be interobserver variability in assessing acromial morphology with MR imaging [29,30].

Other factors aside from acromial morphology may narrow the supraspinatus outlet and thus serve as a substrate for impingement. These include a laterally or anteriorly downsloping acromion, a low-lying acromion, and AC joint separation, or instability (Fig. 9) [18,31].

Coronal oblique and sagittal oblique MR imaging can be used to assess the shape of the acromion and its relationship to the distal clavicle and rotator cuff. The acromioclavicular joint, which is a fibrocartilaginous joint with a central disc, is somewhat immobile, with approximately 20 degrees of movement [6]. Acromioclavicular joint osteoarthritis is extremely common in asymptomatic individuals and is thus not specific for impingement [32]. However, undersurface osteophytes off the acromioclavicular joint can narrow the subacromial space and are thus potential substrates for impingement (Fig. 10). Specifically, the bursal surface of the supraspinatus tendon may be damaged as it moves under the acromioclavicular joint during glenohumeral joint abduction [10].

A normal variant of the acromion, the os acromiale, represents an unfused accessory ossification center of the anterior acromion (Fig. 11) [33]. The diagnosis can be made if there is failure of fusion by age 25. An os acromiale can be a substrate for impingement as a result of hypermobility/instability of the osseous fragment or osseous proliferation at the junction of the os acromiale with the

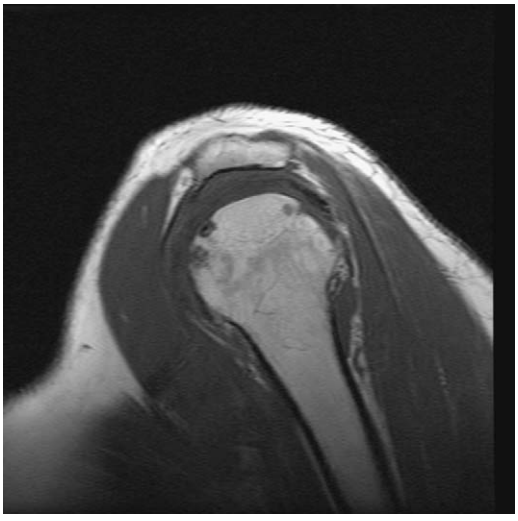

Fig. 8. Acromial morphology. Sagittal oblique T1-weighted images shows anterior acromial spur at insertion of coracoacromial ligament.

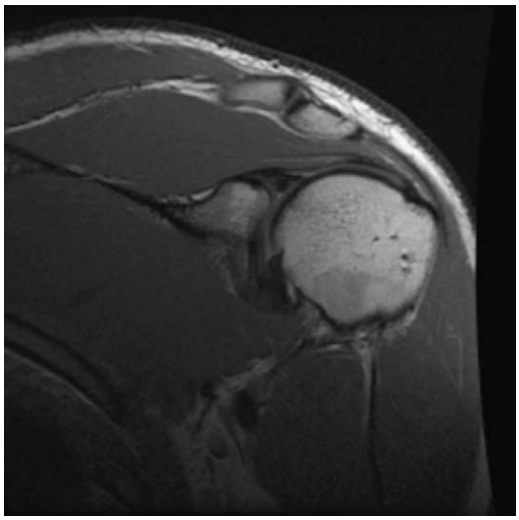

Fig. 9. Acromial position. Coronal oblique proton density image shows laterally downsloping acromion.

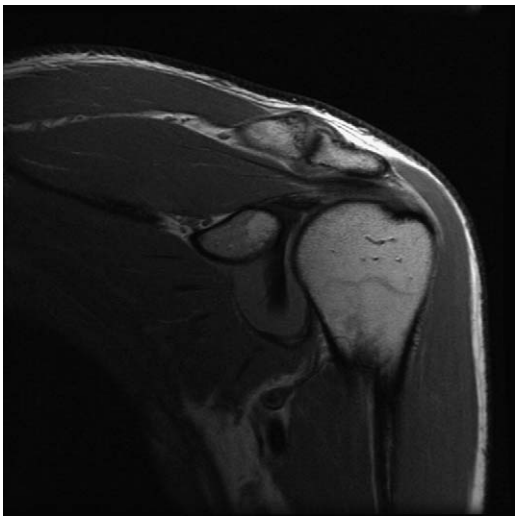

Fig. 10. Acromioclavicular joint. Coronal oblique proton density image shows acromioclavicular joint hypertrophic degenerative change with mass affect on supraspinatus.

remainder of the scapula [34]. The ossicle may be unstable as a result of attachment of the deltoid tendon into the inferior lateral aspect of the ossicle. An os acromiale is important to identify preoperatively as the synchondrosis may be weakened by a subacromial decompression and thus become more mobile. Alternatively, a standard subacromial decompression in the setting of an os acromiale may result in deltoid tendon detachment [35]. There are variable treatments for symptomatic os acromiale, from extended subacromial decompression to internal fixation of the synchondrosis [36].

Fig. 11. Os acromiale. Axial spoiled gradient-echo image shows os acromiale.

Primary extrinsic impingement: subcoracoid

First described in 1985, subcoracoid impingement, also referred to as coracoid impingement, refers to impingement of the subscapular tendon between the coracoid process and the humerus, also known as the coracohumeral interval [11,12,37]. In addition, components of the rotator interval, such as the coracohumeral ligament and the long head biceps brachii tendon, may also become impinged in this location. Entrapment of these structures may lead to degeneration and tearing. The clinical signs of subcoracoid impingement include anterior shoulder pain, which is exacerbated by forward flexion, internal rotation, and cross-arm adduction [38]. Three general etiologies for architectural abnormalities of the coracoid that may lead to subcoracoid impingement have been described: (1) idiopathic enlargement, elongation, or downsloping of the coracoid process; (2) iatrogenic postsurgical deformities of the coracoid; and (3) posttraumatic deformities of the coracoid or lesser tuberosity. The common denominator in these three situations is narrowing of the coracohumeral space. The coracohumeral space, as measured on axial CT or MR imaging, is the distance between the tip of the coracoid process and the lesser tuberosity of the humerus with the arm in internal rotation. In one study, although there was overlap between symptomatic and asymptomatic individuals, the mean coracohumeral distance in patients with subcoracoid impingement was 5.5 mm, whereas that in asymptomatic patients was 11 mm, with none in the latter group having a distance of less than 4 mm [39]. Given these anatomic factors, when abnormalities of the subscapularis tendon and the rotator interval are identified, the coracohumeral space should be carefully evaluated for potential causes of subcoracoid impingement (Fig. 12). Subcoracoid impingement, which may be overlooked at initial evaluation of a patient with an impingement syndrome, may lead to persistent pain following routine rotator cuff surgery [40]. In such patients, treating the abnormalities of the coracoid with coracoplasty was shown to result in complete relief of pain in nine of nine patients who had previously failed prior anterior acromioplasty and rotator cuff repair [40].

Secondary extrinsic impingement

Secondary extrinsic impingement refers to rotator cuff impingement secondary to glenohumeral or, rarely, scapulothoracic instability [10,13]. This type of impingement is typically seen in athletes who participate in sports that require repetitive overhead or throwing motions. In these cases, the coracoacromial arch has a normal configuration

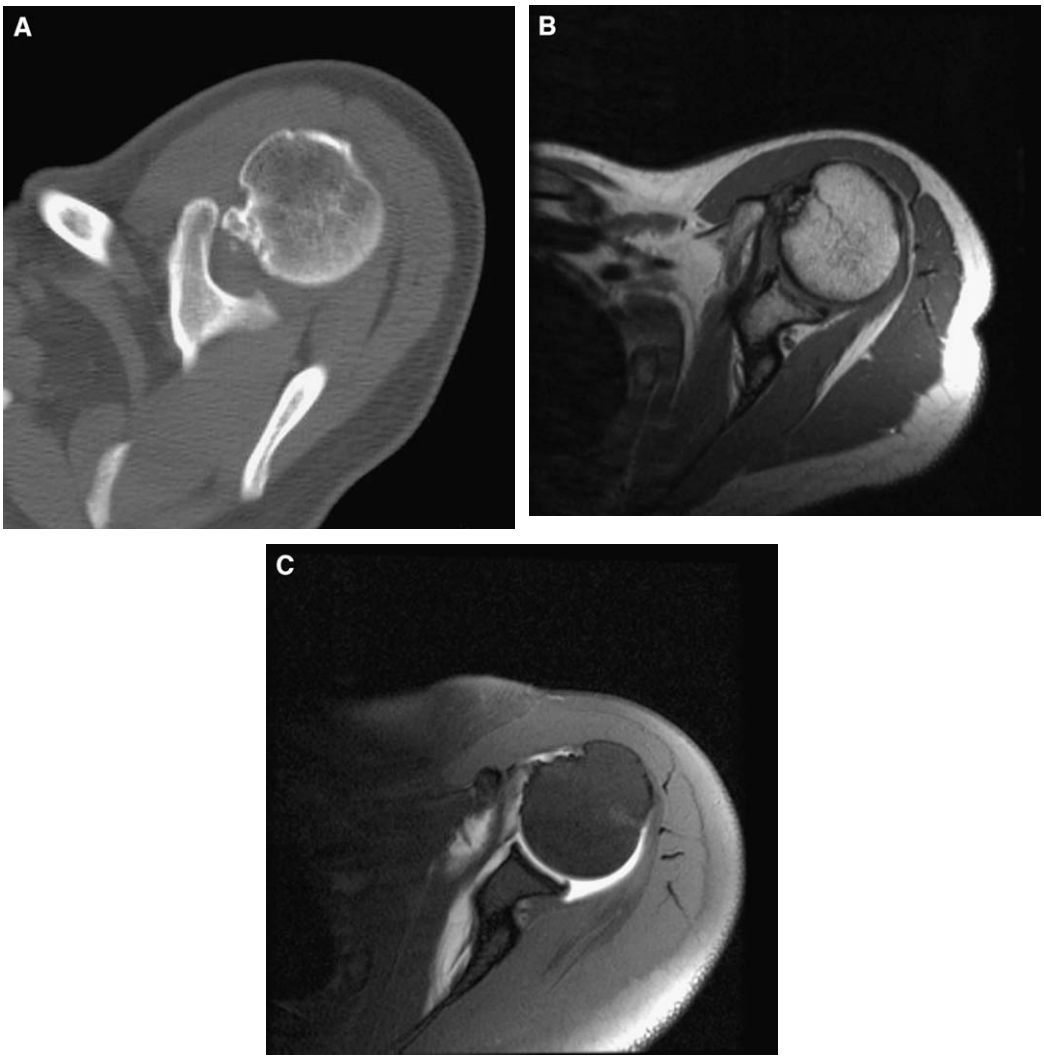

Fig. 12. Subcoracoid impingement. (*A*) axial CT scan shows contact between the tip of the coracoid and the lesser tuberosity, the latter of which is sclerotic and hypertrophied. (*B*) Axial proton density image shows decreased coracohumeral distance with partial tear of the subscapularis muscle as evidenced by expansion and high signal intensity. (*C*) Axial fat-suppressed T1-weighted image from MR arthrogram shows partial tear of the subscapularis tendon.

without any of the previously described abnormalities that may result in primary extrinsic subacromial impingement. On clinical exam, the signs of impingement may predominate and thus mask signs of underlying glenohumeral instability. Examination under anesthesia is helpful in such cases as it allows identification of glenohumeral instability. With instability, superior migration of the humeral head may lead to narrowing of the supraspinatus outlet. In these cases, chronic instability may be a result of weakening of the glenohumeral ligaments and anterior capsule [41]. As these static stabilizers are weakened, more load is placed on dynamic stabilizers, namely, the muscles of the rotator cuff. Such a workload may result in fatigue of the cuff muscles, which thus allows superior migration of the humeral head resulting in a decreased acromiohumeral distance. This type of instability results in impingement of the rotator cuff, which may lead to degeneration and tear of the rotator cuff, particularly on its articular surface along the posterior rotator interval where the supraspinatus and infraspinatus tendons converge (Fig. 13) [42].

Internal impingement

Internal impingement may be classified as posterosuperior impingement or anterosuperior impingement. Posterosuperior impingement refers to

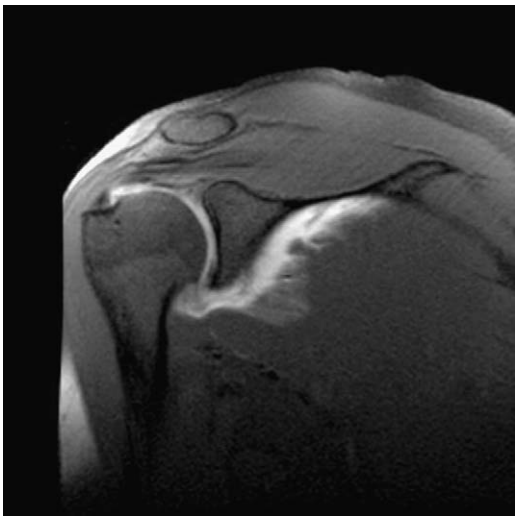

Fig. 13. Partial-thickness rotator cuff tear. Coronal oblique fat-suppressed image from MR arthrogram demonstrates partial-thickness undersurface tear at the junction of the supraspinatus and infraspinatus, a region referred to as the posterior interval.

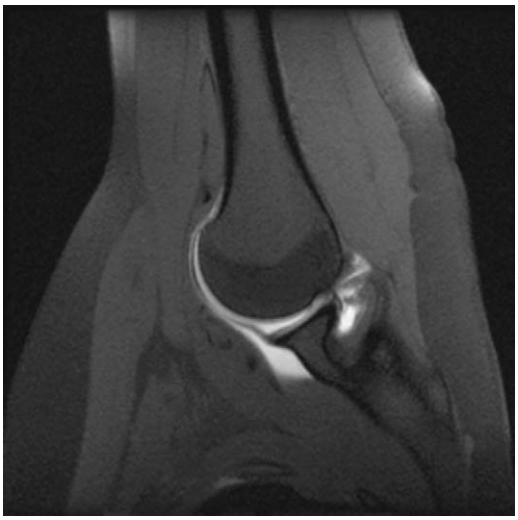

Fig. 14. Posterior superior impingement. MR arthrogram obtained in the ABER position shows posterior superior labral tear, undersurface tear of the supraspinatus, and small defect in humeral head in a patient with posterior superior impingement.

abnormalities caused by friction between the posterosuperior labrum and glenoid and the undersurface of the supraspinatus as the shoulder is moved through the abduction external rotation (ABER) position (Fig. 14) [14]. This type of impingement typically is seen in overhead and throwing athletes and may occur without or with glenohumeral instability. MR imaging demonstrates degeneration and tearing of the posterosuperior glenoid labrum, articular surface fraying, and partial-thickness tearing of the supraspinatus, occasionally as far posteriorly as its junction with the infraspinatus (posterior interval) [43]. Additional findings may include glenoid cysts and osteochondral impaction fractures of the greater tuberosity. Because of the location of these lesions, MR arthrography with the patient in the ABER position provides excellent visualization of the affected regions of the posterosuperior labrum, glenoid, and articular surface of the rotator cuff [44].

A second type of internal impingement has recently been described. Gerber and Sebesta [37] described an impingement of the articular surface fibers of the subscapularis tendon along the anterior superior glenoid rim. In their arthroscopic study, when the glenohumeral joint was flexed and internally rotated, anterior tissues were impinged along the anterior superior glenoid. If the arm was elevated greater than 90 degrees, the long head biceps and the common insertion of the superior glenohumeral ligament and coracohumeral ligament (biceps pulley) was impinged against the superior labrum. With less than 90 degrees elevation, the articular surface fibers of the subscapularis tendon contacted the anterior superior labrum and glenoid rim. None of the patients had signs or symptoms of instability. In 10 of 13 patients with arthroscopically proven partial-thickness subscapularis tears, MR arthrography demonstrated partial articular surface tears of the subscapularis tendon. In another study using nonarthrographic MR imaging, only 20% of arthroscopically proven partial-thickness articular surface tears were identified on MR imaging in the setting of anterosuperior impingement [45].

Rotator cuff tendon abnormalities

Tendinopathy

Classically, rotator cuff tears occur in the insertional fibers of the cuff tendons in regions of preexisting tendinopathy [46]. The etiology of tendinopathy, or tendinosis, is likely multifactorial with contributions from aging, trauma, overuse, and metabolic conditions [10]. The typical MR appearance of tendinopathy is high signal on short TE sequences, such as proton density sequences, which does not become as high as fluid signal on long TE sequences, such as T2-weighted sequences [46]. The signal abnormalities may be seen in the setting of either normal tendon morphology or somewhat thickened tendons. One pitfall to assessing the cuff tendons with short TE imaging is that the magic angle phenomenon may result in artifactually increased signal in regions where the tendon courses at a 55-degree angle in relation to the main

magnetic field. Magic angle artifact should resolve on T2-weighted (long TE) sequences, thus differentiating it from tendinopathy. Additionally, volume averaging between the tendon and adjacent tissues such as muscle, fascia, fat, and cartilage may result in high tendon signal on short TE imaging. Again, use of T2-weighted imaging and assessing tendons in at least two planes can increase confidence in differentiating artifact from true intratendinous signal abnormalities [19,47].

Partial-thickness tears

Partial-thickness rotator cuff tears can be described according to the surface of the tendon involved as well as the percentage of tendon involved. Tears may involve one of three regions of distal tendon fibers: articular surface (aka, undersurface), bursal surface, and intrasubstance. Articular surface tears are the most common type and are easily diagnosed with standard MR imaging when a joint effusion is present. Partial-thickness articular surface tears are characterized by a focal region of fiber discontinuity that is filled with fluid signal as demonstrated on T2-weighted imaging. Fat-suppressed T2-weighted imaging can increase lesion conspicuity by better demonstrating the fluid-filled tendon defect (Fig. 15) [2]. Aside from a focal tendon defect, additional findings may include surface fraying or changes in tendon caliber, such as attenuation or thickening [47]. Tendon retraction is uncommon but may occasionally be seen in high-grade partial-thickness tears. In the absence of a joint effusion, articular surface partial-thickness tears may be difficult to identify, particularly in the setting of granulation tissue or scarring. In one study, the sensitivity, specificity, and accuracy of standard MR imaging for partial tears were 35% to 44%, 85% to 97%, and 77% to 87%, respectively [48]. In these cases, MR arthrography without and with additional imaging in the ABER position has been shown to improve conspicuity of articular surface tears of the rotator cuff (Fig. 16) [44,49–51]. Two recent studies demonstrated MR arthrography to be 84% to 95% sensitive and 96% to 100% specific for partial-thickness articular surface tears of the rotator cuff [52,53]. Intrasubstance tears are characterized by intratendinous T2 fluid signal without extension to either the bursal or articular surface (Fig. 17). These lesions will not fill with gadolinium on MR arthrography because of lack of communication between the tear and the articular surface of the tendon. Intrasubstance tears may be occult on tendon visualization during arthroscopic or open surgery because of intact tendon surfaces. However, careful probing may demonstrate the focal tendon abnormality.

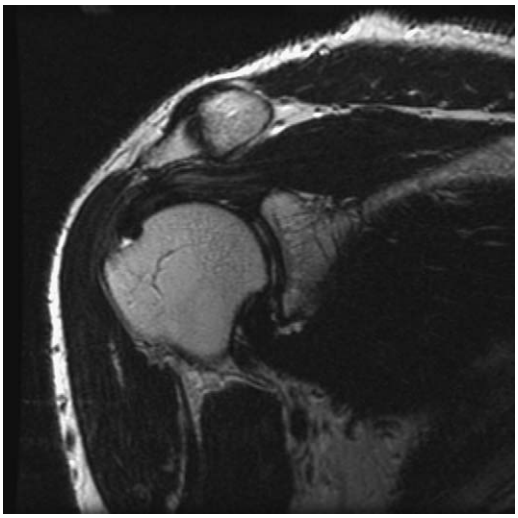

Fig. 15. Partial-thickness rotator cuff tear. Coronal T2-weighted image shows partial thickness articular surface tear of the supraspinatus.

Partial-thickness bursal surface tears result in discontinuity of the tendon along its superior (bursal) surface with an extraarticular fluid-filled gap. The articular surface remains intact. When there is fluid in the subacromial bursa, the tears are well visualized, particularly on T2-weighted images. However, these tears may not be visible on T1-weighted MR arthrographic images as the intraarticular gadolinium will not enter the gap in the tendon because of intact articular surface fibers. In addition, the presence of bursal fluid may not be appreciated on T1-weighted imaging (Fig. 18). For these reasons, it is crucial to include at least one T2-weighted sequence on all MR arthrographic exams to assess for fluid-filled bursal surface tears. These T2-weighted images are also useful for assessing other periarticular fluid collections and cysts that may be occult on T1-weighted imaging. Although rarely performed, bursal injection of gadolinium for direct MR bursography can be performed to outline bursal surface partial-thickness rotator cuff tears [54].

Partial-thickness rotator cuff tears have been classified arthroscopically according to the degree of tendon involvement [55,56]. Grade 1 lesions involve less than 25% of the tendon thickness (less than 3 mm); grade 2 lesions involve 25% to 50% (3 to 6 mm); and grade 3 lesions involve greater than 50% of the tendon (greater than 6 mm). In the end, surgical treatment, including debridement versus actual cuff repair, depends on degree of tearing, tendon quality, and activity level of the patient [57].

Full-thickness tears

When a tear of the rotator cuff results in a discontinuity in the tendon that extends from the articular

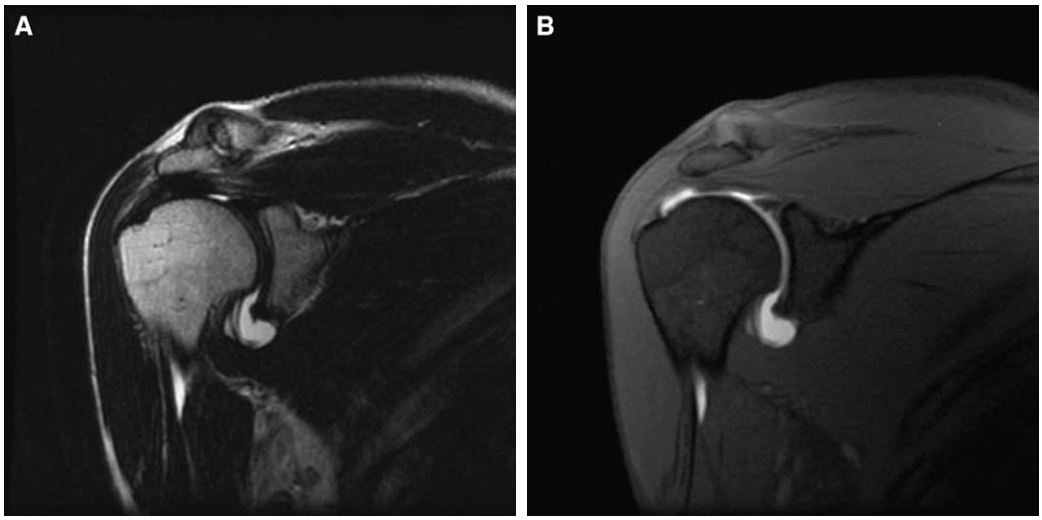

Fig. 16. Partial-thickness tear not visible on T2-weighted imaging. (*A*) Coronal oblique T2-weighted image shows thickening of the distal supraspinatus tendon without specific evidence for a rotator cuff tear. (*B*) Coronal oblique T1-weighted fat-suppressed image from MR arthrogram in the same patient shows partial-thickness articular surface tear not visible on T2-weighted imaging.

surface to the bursal surface, it is referred to as a full-thickness tear (Fig. 19). Full-thickness tears can be classified according to the size of the tear: small (less than 1 cm), medium (1 to 3 cm), large (3 to 5 cm), and massive (greater than 5 cm). Massive tears of the rotator cuff involve supraspinatus and infraspinatus and are usually associated with tendon retraction. Supraspinatus tears that are greater than 2.5 cm in anteroposterior dimension often extend into the infraspinatus or the subscapularis. The tear does not need to involve the entire tendon in an anteroposterior dimension to be considered a full-thickness tear. Conventional nonarthrographic MR imaging is an accurate test for depicting full-thickness tears of the rotator cuff. Although fat-suppressed imaging may increase sensitivity for full-thickness tears, there is no significant change in specificity [2]. The characteristic and most specific sign of a full-thickness rotator cuff tear is tendon discontinuity [58]. The presence of fluid in the subacromial-subdeltoid bursa, although not specific for a full-thickness tear, is considered by some authors to be the most sensitive sign [58]. In one study, the sensitivity, specificity, and accuracy of MR imaging for full-thickness rotator cuff tears were 84% to 96%, 94% to 98%, and 92% to 97%, respectively [48]. Recently, MR arthrography was shown to be 98% sensitive and 100% specific for partial-thickness articular surface rotator cuff tears, with 100% accuracy for full-thickness tears [52]. MR arthrography may demonstrate a small full- thickness component of a rotator cuff tear that may appear as being only a partial-thickness tear on standard MR imaging (Fig. 20). When evaluating rotator cuff tears, the anteroposterior and mediolateral (ie, tendon retraction) measurements as well as the quality of torn tendon margin should be described in the report as these factors are valuable to the surgeon when assessing prognosis and planning surgery (arthroscopic versus open) [59].

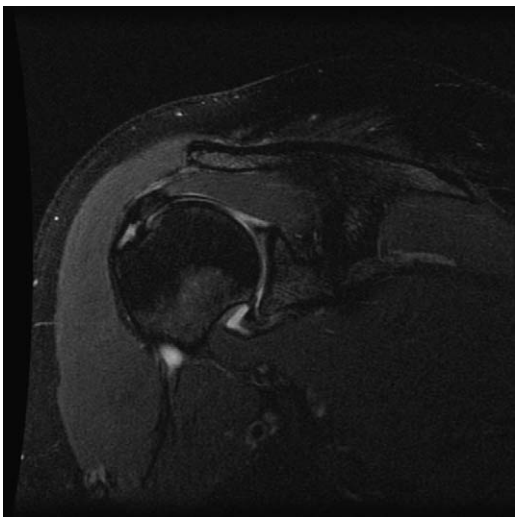

Fig. 17. Partial-thickness rotator cuff tear. Coronal oblique fat-suppressed T2-weighted image shows intrasubstance tear of the supraspinatus with normal articular and bursal surfaces.

Although rotator cuff tears typically appear as areas of fluid signal intensity on T2-weighted images, in about 10% of tears, the region of tendon

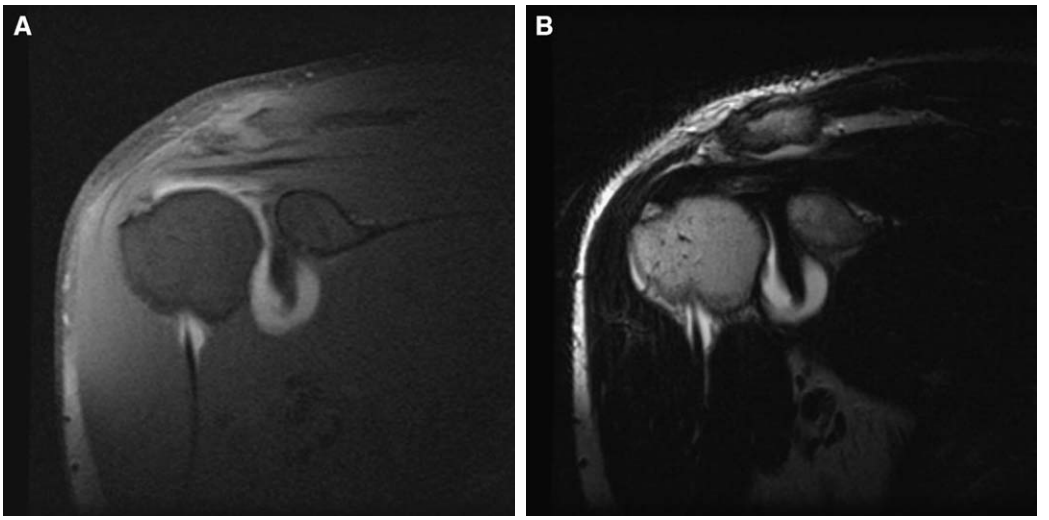

Fig. 18. Bursal surface tear not visible on T1-weighted images from MR arthrogram. (*A*) Coronal oblique fat-suppressed T1-weighted image shows a normal rotator cuff. (*B*) T2-weighted image at same level shows partial-thickness bursal surface tear of the supraspinatus.

discontinuity is low in signal on T2-weighted images, possibly because of chronic scarring (Fig. 21A) [47]. These tears may be visualized at MR arthrography because intraarticular contrast fills the tear (Fig. 21B). On conventional MR imaging, secondary signs of cuff tear, such as tendon retraction, may be the only indication of a full-thickness tear. The normal myotendinous junction should lie within a 15-degree arc of the 12 o'clock position of the humeral head on coronal oblique imaging [58]. Thus, if the myotendinous junction is more than 15 degrees medial to the 12 o'clock position, there may be a full-thickness cuff tear. In addition, if there is superior translation of the humeral head with associated remodeling of the undersurface of the acromion, one should suspect a full-thickness tear with retraction, which resulted in acromiohumeral articulation (Fig. 22). Although muscle atrophy may be seen in the setting of rotator cuff tears and usually indicates chronicity, there may be other, although less common, causes for muscle atrophy in the setting of an intact cuff. Muscle atrophy represents an important component in managing rotator cuff tears as it may determine surgical approach (open versus arthroscopic) and may be a predictor of operative success (Fig. 23) [59]. Muscle atrophy is best depicted on T1 weighted, particularly in the sagittal oblique plane. MR imaging has been proposed as a method for quantifying degree of muscle atrophy [60]. Alternatively, preliminary work suggests that early metabolic changes associated with muscle atrophy may be detected by MR spectroscopy despite normal morphology of a muscle on MR imaging (M. Torriani, personal communication, September 2003).

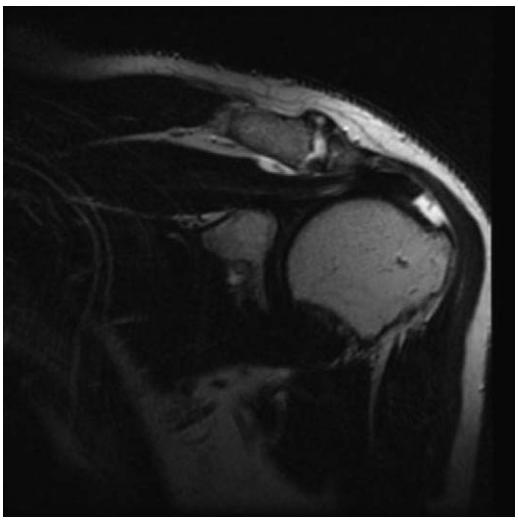

Fig. 19. Full-thickness rotator cuff tear. Coronal oblique T2-weighted image shows full-thickness supraspinatus tear with tendon retraction and a fluid-filled gap.

Two types of periarticular cysts have been reported to be associated with rotator cuff tear [61,62]. An acromioclavicular joint cyst likely develops from leakage of fluid from the glenohumeral joint through a full-thickness rotator cuff tear into a degenerated acromioclavicular joint (Fig. 24). The presence of such a cyst, which communicates with the glenohumeral joint, a finding that can be confirmed by MR arthrography, may require distal

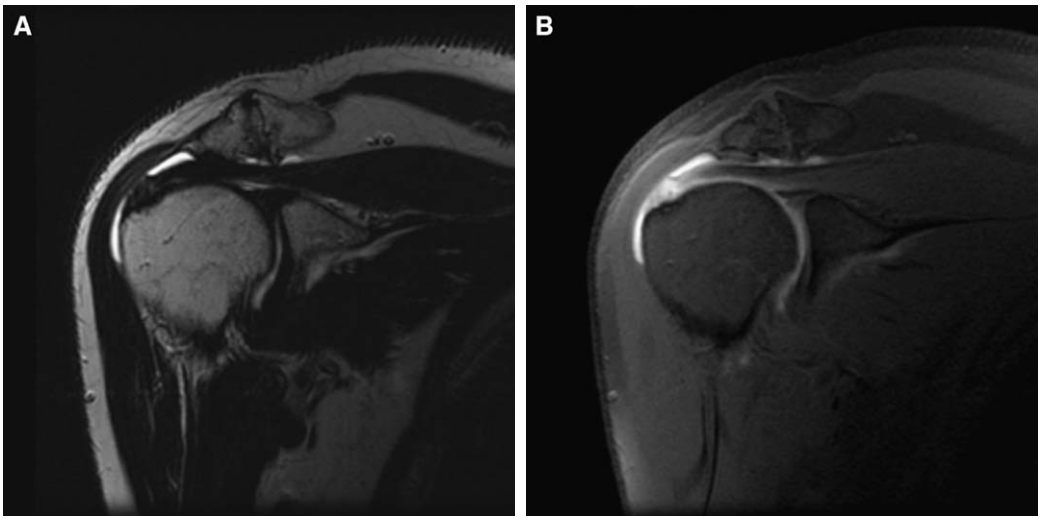

Fig. 20. Full-thickness rotator cuff tear not visible on T2-weighted image. (*A*) Coronal oblique T2-weighted image shows fluid in the subdeltoid bursa without evidence of full-thickness supraspinatus tear. (*B*) Coronal oblique fat-suppressed T1-weighted at same level shows gadolinium traversing full-thickness tear with gadolinium in the subdeltoid bursa.

clavicular resection in addition to acromioplasty at the time of rotator cuff repair to avoid cyst recurrence [61]. If no such communication exists with the glenohumeral joint on MR arthrography, the cyst is less likely to recur following local excision without distal clavicular resection. Intramuscular cysts, or ganglia, are formed as fluid from the glenohumeral joint dissects along the rotator cuff muscle either along the fascial sheath or within the substance of the muscle, typically along the myotendinous plane (Fig. 25). The presence of such an intramuscular fluid collection has been associated with small full-thickness or articular surface partial-thickness tears of the rotator cuff and should thus prompt a meticulous search for rotator cuff tears [62].

In the setting of a chronic supraspinatus tear, the long head biceps brachii tendon may become impinged between the humeral head and the acromion [10]. Thus, tendinopathy or tears of the intracapsular portion of the long head biceps tendon may be seen associated with supraspinatus tears. If the rotator cuff tear extends to and involves the rotator interval and subscapularis, the biceps tendon may dislocate out of the bicipital groove

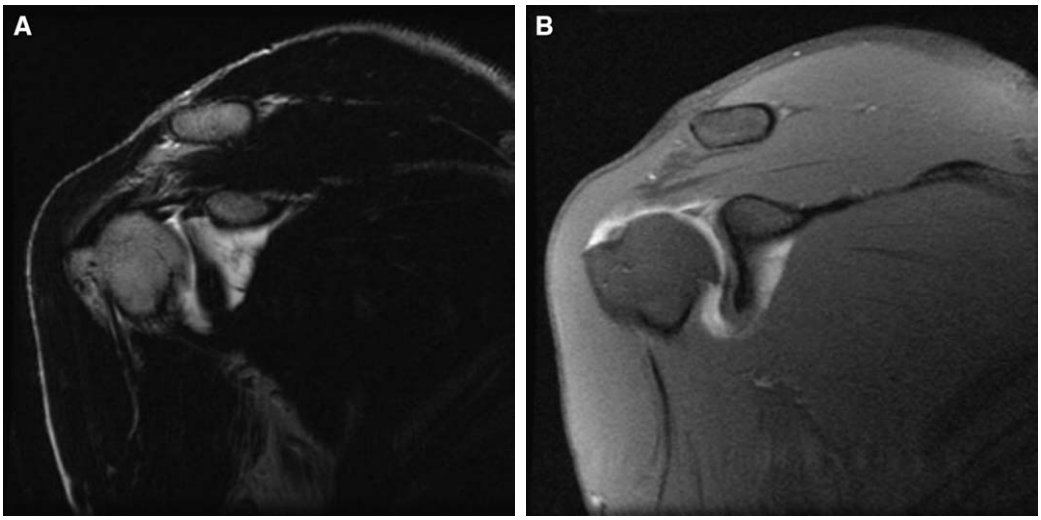

Fig. 21. T2 dark rotator cuff tear. (*A*) Coronal oblique T2-weighted image shows a normal supraspinatus tendon. (*B*) Coronal oblique fat-suppressed T1-weighted image shows near full-thickness tear of supraspinatus.

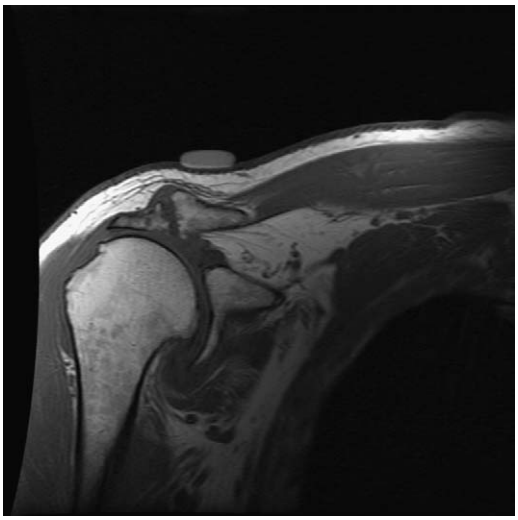

Fig. 22. Acromiohumeral articulation. Coronal oblique proton density image shows full-thickness supraspinatus tear with retraction and atrophy resulting in acromiohumeral articulation and remodeling of undersurface of acromion.

(see article on biceps/interval in this issue of MR clinics) [63].

Identification of subscapularis tear can be challenging clinically and surgically [64]. Imaging plays a crucial role in preoperative identification of such tears as their presence may affect surgical planning. Typically, traumatic subscapularis tears involve the cranial fibers with the caudal fibers being involved in extensive tears. Isolated tears of the caudal fibers of the subscapularis are rare [65]. Subscapularis injuries typically follow one of three patterns: (1) isolated subscapularis tear; (2) subscapularis tear in the setting of a large rotator cuff tear; and (3) subscapularis tear in the setting of anterosuperior lesions of the rotator cuff. Isolated full-thickness subscapularis tears are uncommon and typically occur in the setting of acute trauma, often the result of forced external rotation of an adducted arm, forceful extreme abduction and external rotation, anterior dislocation, or recurrent anterior glenohumeral instability. A far more frequent situation is extension of a supraspinatus tear into the subscapularis [64]. Anterior superior lesions of the rotator cuff involve the most anterior fibers of the supraspinatus, the cranial fibers of the subscapularis, and the intervening components of the rotator interval, the coracohumeral and superior glenohumeral ligaments [66]. The diagnosis of subscapularis tear on MR imaging is based on the identification of tendon discontinuity, gadolinium filling a gap over the lesser tuberosity, atrophy of the subscapularis, or malposition of the tendon of the long head biceps brachii (Fig. 26) [64]. These findings are best seen on axial and oblique sagittal images. Aside from tendon discontinuity, the remaining signs are reported to be specific but not sensitive on MR arthrography for the diagnosis of subscapularis tears. In skeletally immature patients, an avulsion injury of the lesser tuberosity, often associated with a tear of the anterior band of the inferior glenohumeral ligament, may be seen (Fig. 27) [67,68]. As with most tendon injuries, subscapularis tears are treated differently depending on the extent of the lesion and the functional demand of the

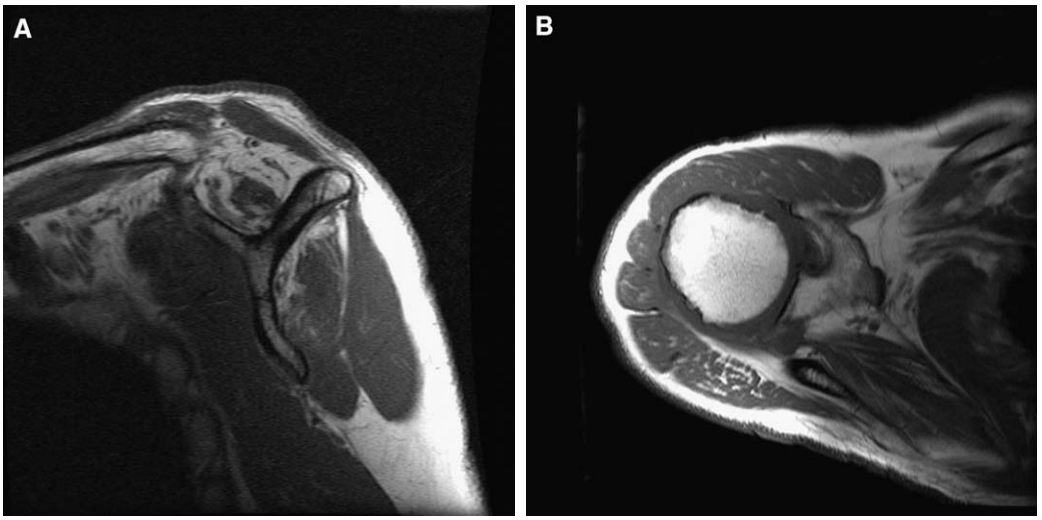

Fig. 23. Full-thickness tear with retraction and atrophy. (*A*) Sagittal oblique T1-weighted image shows atrophic supraspinatus muscle. (*B*) Axial T1-weighted image shows retraction of myotendinous junction medial to glenoid.

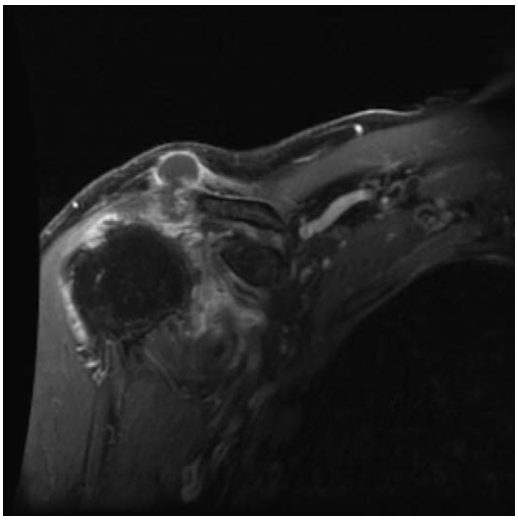

Fig. 24. Acromioclavicular joint cyst communicating with glenohumeral joint. Coronal oblique fat-suppressed T1-weighted image following administration of intravenous gadolinium demonstrates full-thickness rotator cuff tear with atrophy. There is communication between glenohumeral joint and large acromioclavicular cyst, which demonstrates peripheral enhancement.

patient. In patients with low functional demand, physical therapy, pain control, and steroid injections may be sufficient. Small degenerative tears and large inoperable tears may be treated with arthroscopic debridement for symptomatic relief. Patients with high functional demand generally require reconstruction with arthroscopic or open surgery either by direct tendon repair or with a pectoralis major tendon transfer [69].

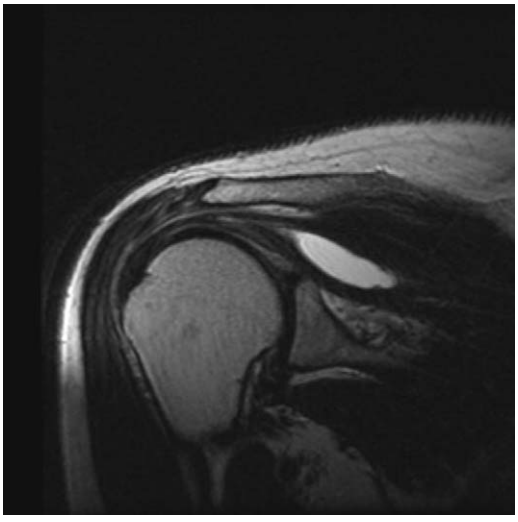

Fig. 25. Intramuscular cyst. Coronal oblique T2-weighted image shows intramuscular ganglion or cyst within the infraspinatus muscle.

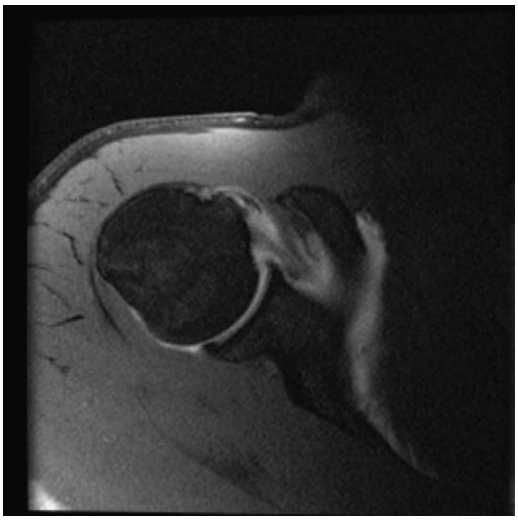

Fig. 26. Biceps tendon dislocation. Axial fat-suppressed T1-weighted image from MR arthrogram shows a split tear of subscapularis with intratendinous dislocation long head biceps brachii tendon.

In approximately 8% to 10% of cases, a rotator cuff tear is caused by acute injury to an otherwise healthy tendon (Fig. 28) [70]. Patients under the age of 40 who have an acute traumatic event and are suspected of having an acute rotator cuff tear are at risk of having an undisplaced greater tuberosity fracture. Such fractures are often treated conservatively as the periosteum is thought to stabilize the fracture and thus aid in healing without the need for rotator cuff surgery [71]. In the same series, patients over 40 with a suspicion of acute rotator cuff injury had a high prevalence of subscapularis tears. Thus, in the setting of acute trauma, special attention should be paid to the greater tuberosity and the subscapularis tendon.

Rotator interval tears

The rotator interval lies between the anterior fibers of the supraspinatus and the cranial fibers of the subscapularis. Although the anatomy and pathophysiology of the rotator interval is discussed in detail elsewhere in this issue, one must be sure to evaluate the rotator interval in all cases of anterior supraspinatus tears, cranial subscapularis tears, biceps tendon abnormalities, and subcoracoid bursal effusions or bursitis [72]. The rotator interval is best evaluated on sagittal oblique images, particularly with MR arthrography.

Mimics of rotator cuff tears

Greater tuberosity fractures may mimic a rotator cuff tear. These fractures are often nondisplaced fractures that are radiographically occult (Fig. 29).

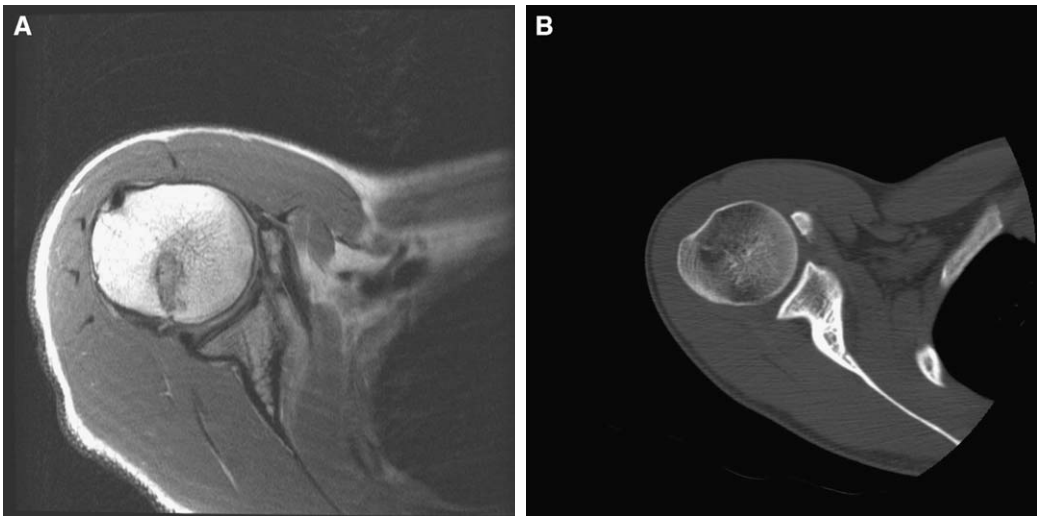

Fig. 27. Lesser tuberosity avulsion. (*A*) Axial proton density-weighted image in an adolescent shows flattening of lesser tuberosity and clearly defines relationship of the intact subscapularis tendon and the avulsed fragment of bone. (*B*) Axial CT scan shows ossific fragment anterior to humerus with some flattening of the lesser tuberosity.

The mechanism for these fractures is often either shoulder dislocation or impaction of the greater tuberosity and the acromion during forced abduction. Using the Neer classification, these are one-part fractures and usually do not need surgical treatment [73]. These patients are often referred to MR imaging for suspected rotator cuff tears. In one series that included MR imaging of 12 patients with acute traumatic radiographically occult greater tuberosity fractures, all 12 patients had either tendinosis or partial-thickness cuff tears without any full-thickness cuff component [74]. All patients were treated nonoperatively. The authors postulated that the greater tuberosity fracture precluded a full-thickness rotator cuff tear. If one is to treat a rotator cuff tear associated with a greater tuberosity fracture, one must postpone surgery to allow fracture healing to ensure subsequent successful cuff repair [71].

Distal clavicular osteolysis may be seen in acute injury or following repeated stress-related microtrauma to the acromioclavicular joint. The latter

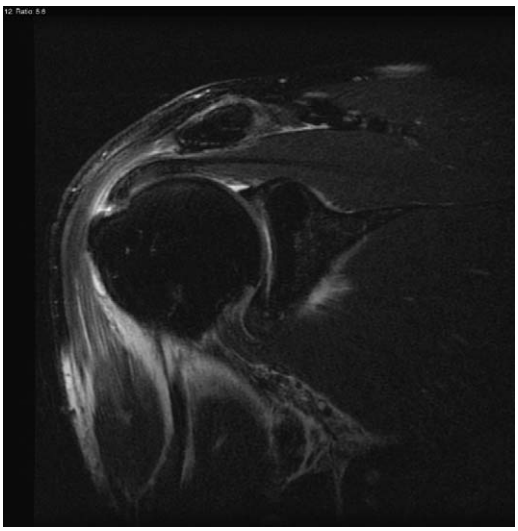

Fig. 28. Acute full-thickness rotator cuff tear. Coronal oblique fat-suppressed intermediate-weighted image show acute full-thickness supraspinatus tear with associated edema in surrounding tissues.

Fig. 29. Greater tuberosity fracture. Coronal oblique proton density image show avulsion of the greater tuberosity in a patient suspected of having rotator cuff tear.

may be related to athletic or work-related activities. Distal clavicular osteolysis manifests radiographically as resorption of the distal clavicle with loss of the distal clavicular cortical line and pseudo widening of the acromioclavicular joint [75]. The most common finding on MR imaging is edema, predominantly in the distal clavicle. As with most types of edema, this is best demonstrated on fat-suppressed T2 or inversion recovery imaging (Fig. 30). Additional features include acromioclavicular joint fluid, distention of the joint capsule, and cortical irregularity without or with fragmentation of the distal clavicle [75].

Muscle weakness secondary to denervation or neuritis may mimic rotator cuff tears. This typically occurs when the suprascapular nerve, which innervates the supraspinatus and infraspinatus, is affected. The suprascapular nerve may be compromised as a result of trauma, inflammation, or compression. In the setting of acute trauma, a scapular fracture may be associated with suprascapular nerve injury. Alternatively, the nerve may experience a stretch injury, often in the setting of a brachial plexus injury or other distraction type injury. One cadaveric study demonstrated stretching of the suprascapular nerve at the level of the spinoglenoid notch as the glenohumeral joint was moved into a cross-body adduction and internal rotation position [76]. Volleyball players, particularly those who use a "float" serve, may have selective infraspinatus atrophy caused by stretch injury of the suprascapular nerve at the level of the spinoglenoid notch [8]. This is thought to result from a strong eccentric contraction of the infraspinatus that is required to quickly retract the arm immediately following contact with the ball. In addition, a stretching injury of the axillary nerve in the setting of an anterior shoulder dislocation may result in selective teres minor atrophy [77]. Neuritis, or nerve inflammation, may have many etiologies, including postviral neuritis. Acute brachial neuritis, also known as Parsonage-Turner syndrome, may result in atraumatic shoulder pain and weakness, thereby mimicking a rotator cuff tear [78]. Although the pain may resolve in 1 to 3 weeks, weakness of the affected muscles may persist and result in atrophy. Although the supraspinatus and infraspinatus are typically affected, the deltoid and rhomboids may also be affected [79]. Finally, compression of the suprascapular nerve may result in denervation. Although this is typically caused by paralabral cysts, any strategically located space-occupying lesion may cause compression of the suprascapular nerve (Fig. 31). If the lesion is located along the course of the suprascapular nerve proximal to the spinoglenoid notch, both the supraspinatus and infraspinatus will be affected, whereas a lesion at or distal to the spinoglenoid notch will selectively affect the infraspinatus.

Regardless of the cause, neural compromise may result in interstitial denervation edema, which is well depicted on fluid-sensitive sequences, such as fat-suppressed T2 or inversion recovery [80]. At later stages, muscle atrophy may be present. In an experimental study, such edema was present on inversion recovery imaging at 24 hours following

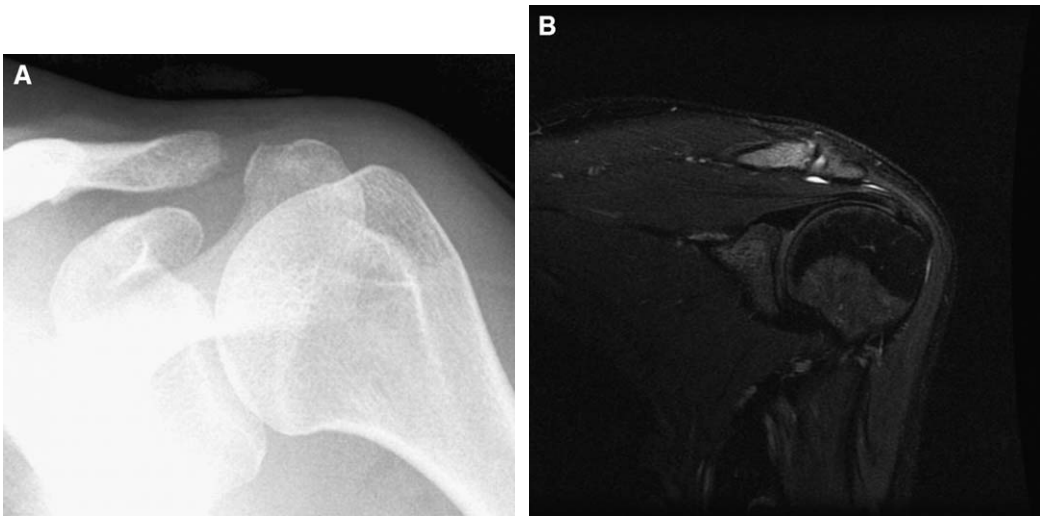

Fig. 30. Posttraumatic osteolysis of the distal clavicle. (*A*) Magnified view from shoulder radiograph 3 weeks following acute trauma shows subtle osteolysis of distal clavicle with loss of cortical line. Note normal acromial cortical line. (*B*) Coronal oblique fat-suppressed intermediate weighted image shows mild edema in the distal clavicle and indistinct cortical margin.

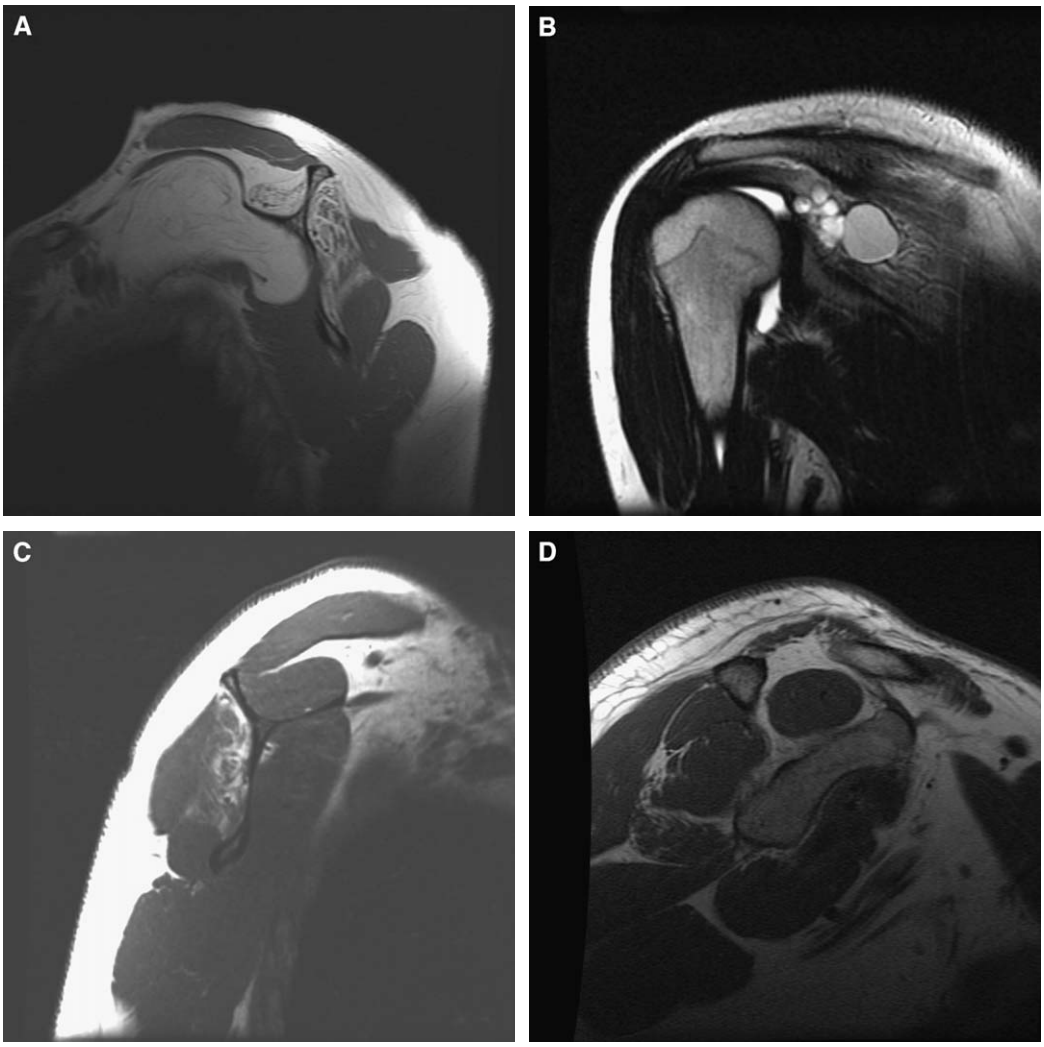

Fig. 31. Rotator cuff muscle atrophy with intact tendons. (*A*) Sagittal oblique T1-weighted image shows large lipoma compressing suprascapular nerve resulting in atrophy of the supraspinatus and infraspinatus. (*B*) Coronal oblique T2-weighted image shows multiloculated cyst in spinoglenoid notch resulting in selective infraspinatus atrophy. (*C*) Sagittal oblique T1-weighted image in same patient shows selective infraspinatus atrophy. (*D*) Sagittal oblique T1-weighted image in a different patient shows selective teres minor atrophy following anterior shoulder dislocation.

denervation, and atrophy was visible on T1-weighted images as early as 7 days following denervation [81]. Muscle atrophy in the absence of a rotator cuff tear should prompt a search for neural compromise.

Summary

MR imaging is an exquisite tool for delineating normal structures and abnormalities of the rotator cuff and for determining the location and extent of rotator cuff tears before surgery. Although standard MR imaging can accurately demonstrate full-thickness rotator cuff tears and some partial-thickness tears, MR arthrography can increase diagnostic accuracy in small partial-thickness articular surface tears. MR imaging helps to distinguish between many other causes of shoulder pain that may mimic rotator cuff tears.

References

[1] Hawkins RJ, Hobeika PE. Impingement syndrome in the athletic shoulder. Clin Sports Med 1983;2(2):391–405.
[2] Reinus WR, Shady KL, Mirowitz SA, Totty WG. MR diagnosis of rotator cuff tears of the

shoulder: value of using T2-weighted fat-saturated images. AJR Am J Roentgenol 1995; 164(6):1451–5.
[3] Seeger LL, Gold RH, Bassett LW, Ellman H. Shoulder impingement syndrome: MR findings in 53 shoulders. AJR Am J Roentgenol 1988; 150(2):343–7.
[4] Tirman PF, Bost FW, Steinbach LS, Mall JC, Peterfy CG, Sampson TG, et al. MR arthrographic depiction of tears of the rotator cuff: benefit of abduction and external rotation of the arm. Radiology 1994;192(3):851–6.
[5] Hollingshead WH, Rosse C. Textbook of anatomy. Fourth edition. Philadelphia: Harper & Row; 1985. p. 199–201.
[6] Petersilge CA, Witte DH, Sewell BO, Bosch E, Resnick D. Normal regional anatomy of the shoulder. Magn Reson Imaging Clin N Am 1993;1(1):1–18.
[7] Neumann CH, Holt RG, Steinbach LS, Jahnke AH Jr, Petersen SA. MR imaging of the shoulder: appearance of the supraspinatus tendon in asymptomatic volunteers. AJR Am J Roentgenol 1992;158(6):1281–7.
[8] Ferretti A, De Carli A, Fontana M. Injury of the suprascapular nerve at the spinoglenoid notch. The natural history of infraspinatus atrophy in volleyball players. Am J Sports Med 1998; 26(6):759–63.
[9] Beltran J, Bencardino J, Padron M, Shankman S, Beltran L, Ozkarahan G. The middle glenohumeral ligament: normal anatomy, variants and pathology. Skeletal Radiol 2002;31(5):253–62.
[10] Steinbach LS. Rotator cuff disease. In: Steinbach LS, Tirman PFJ, Peterfy CG, Feller JF, editors. Shoulder magnetic resonance imaging. Philadelphia: Lippincott Williams & Wilkins; 1988. p. 99–133.
[11] Gerber C, Terrier F, Ganz R. The role of the coracoid process in the chronic impingement syndrome. J Bone Joint Surg Br 1985;67(5): 703–8.
[12] Ferrick MR. Coracoid impingment. A case report and review of the literature. Am J Sports Med 2000;28(1):117–9.
[13] Jobe FW, Kvitne RS, Giangarra CE. Shoulder pain in the overhand or throwing athlete. The relationship of anterior instability and rotator cuff impingement. Orthop Rev 1989;18(9): 963–75.
[14] Walch G, Liotard JP, Boileau P, Noel E. Posterosuperior glenoid impingement. Another shoulder impingement. Rev Chir Orthop Reparatrice Appar Mot 1991;77(8):571–4.
[15] Boenisch U, Lembcke O, Naumann T. Classification, clinical findings and operative treatment of degenerative and posttraumatic shoulder disease: what do we really need to know from an imaging report to establish a treatment strategy? Eur J Radiol 2000;35(2):103–18.
[16] Wright RW, Fritts HM, Tierney GS, Buss DD. MR imaging of the shoulder after an impingement test: how long to wait. AJR Am J Roentgenol 1998;171(3):769–73.
[17] Beaulieu CF, Hodge DK, Bergman AG, Butts K, Daniel BL, Napper CL, et al. Glenohumeral relationships during physiologic shoulder motion and stress testing: initial experience with open MR imaging and active imaging-plane registration. Radiology 1999;212(3):699–705.
[18] Gallino M, Battiston B, Annaratone G, Terragnoli F. Coracoacromial ligament: a comparative arthroscopic and anatomic study. Arthroscopy 1995;11(5):564–7.
[19] Kaplan PA, Bryans KC, Davick JP, Otte M, Stinson WW, Dussault RG. MR imaging of the normal shoulder: variants and pitfalls. Radiology 1992;184(2):519–24.
[20] Ogata S, Uhthoff HK. Acromial enthesopathy and rotator cuff tear. A radiologic and histologic postmortem investigation of the coracoacromial arch. Clin Orthop 1990;254:39–48.
[21] Ozaki J, Fujimoto S, Nakagawa Y, Masuhara K, Tamai S. Tears of the rotator cuff of the shoulder associated with pathological changes in the acromion. A study in cadavera. J Bone Joint Surg Am 1988;70(8):1224–30.
[22] Bigliani LU, Ticker JB, Flatow EL, Soslowsky LJ, Mow VC. The relationship of acromial architecture to rotator cuff disease. Clin Sports Med 1991;10(4):823–38.
[23] von Schroeder HP, Kuiper SD, Botte MJ. Osseous anatomy of the scapula. Clin Orthop 2001; 383:131–9.
[24] Getz JD, Recht MP, Piraino DW, Schils JP, Latimer BM, Jellema LM, et al. Acromial morphology: relation to sex, age, symmetry, and subacromial enthesophytes. Radiology 1996; 199(3):737–42.
[25] Morrison DS, Bigliani LU. The clinical significance of variation in acromial morphology. Orthop Trans 1986;11:234.
[26] Bigliani LU, Morrison DS, April EW. The morphology of the acromion and its relationship to rotator cuff tears. Orthop Trans 1986; 10:228.
[27] Edelson JG. The 'hooked' acromion revisited. J Bone Joint Surg Br 1995;77(2):284–7.
[28] Shah NN, Bayliss NC, Malcolm A. Shape of the acromion: congenital or acquired—a macroscopic, radiographic, and microscopic study of acromion. J Shoulder Elbow Surg 2001; 10(4):309–16.
[29] Haygood TM, Langlotz CP, Kneeland JB, Iannotti JP, Williams GR Jr, Dalinka MK. Categorization of acromial shape: interobserver variability with MR imaging and conventional radiography. AJR Am J Roentgenol 1994; 162(6):1377–82.
[30] Peh WC, Farmer TH, Totty WG. Acromial arch shape: assessment with MR imaging. Radiology 1995;195(2):501–5.
[31] Banas MP, Miller RJ, Totterman S. Relationship between the lateral acromion angle and rotator

cuff disease. J Shoulder Elbow Surg 1995; 4(6):454–61.
[32] Needell SD, Zlatkin MB, Sher JS, Murphy BJ, Uribe JW. MR imaging of the rotator cuff: peritendinous and bone abnormalities in an asymptomatic population. AJR Am J Roentgenol 1996; 166(4):863–7.
[33] Sammarco VJ. Os acromiale: frequency, anatomy, and clinical implications. J Bone Joint Surg Am 2000;82(3):394–400.
[34] Sterling JC, Meyers MC, Chesshir W, Calvo RD. Os acromiale in a baseball catcher. Med Sci Sports Exerc 1995;27(6):795–9.
[35] Wright RW, Heller MA, Quick DC, Buss DD. Arthroscopic decompression for impingement syndrome secondary to an unstable os acromiale. Arthroscopy 2000;16(6):595–9.
[36] Ryu RK, Fan RS, Dunbar WH 5th. The treatment of symptomatic os acromiale. Orthopedics 1999; 22(3):325–8.
[37] Gerber C, Sebesta A. Impingement of the deep surface of the subscapularis tendon and the reflection pulley on the anterosuperior glenoid rim: a preliminary report. J Shoulder Elbow Surg 2000;9(6):483–90.
[38] Bigliani LU, Levine WN. Subcoracoid impingement syndrome [current concepts review]. J Bone Joint Surg Am 1997;79:1854–68.
[39] Friedman RJ, Bonutti PM, Genez B. Cine magnetic resonance imaging of the subcoracoid region. Orthopedics 1998;21(5):545–8.
[40] Suenaga N, Minami A, Kaneda K. Postoperative subcoracoid impingement syndrome in patients with rotator cuff tear. J Shoulder Elbow Surg 2000;9(4):275–8.
[41] Warner JJ, Micheli LJ, Arslanian LE, Kennedy J, Kennedy R. Patterns of flexibility, laxity, and strength in normal shoulders and shoulders with instability and impingement. Am J Sports Med 1990;18(4):366–75.
[42] Nakagawa S, Yoneda M, Hayashida K, et al. The posterior rotator interval may be the initial site of rotator cuff tears in baseball players. J Shoulder Elbow Surg 1997;6:S246.
[43] Paley KJ, Jobe FW, Pink MM, Kvitne RS, ElAttrache NS. Arthroscopic findings in the overhand throwing athlete: evidence for posterior internal impingement of the rotator cuff. Arthroscopy 2000;16(1):35–40.
[44] Tirman PF, Bost FW, Garvin GJ, Peterfy CG, Mall JC, Steinbach LS, et al. Posterosuperior glenoid impingement of the shoulder: findings at MR imaging and MR arthrography with arthroscopic correlation. Radiology 1994;193(2): 431–6.
[45] Struhl S. Anterior internal impingement. An arthroscopic observation. Arthroscopy 2002; 18(1):2–7.
[46] Kjellin I, Ho CP, Cervilla V, Haghighi P, Kerr R, Vangness CT, et al. Alterations in the supraspinatus tendon at MR imaging: correlation with histopathologic findings in cadavers. Radiology 1991;181(3):837–41.
[47] Rafii M, Firooznia H, Sherman O, Minkoff J, Weinreb J, Golimbu C, et al. Rotator cuff lesions: signal patterns at MR imaging. Radiology 1990; 177(3):817–23.
[48] Balich SM, Sheley RC, Brown TR, Sauser DD, Quinn SF. MR imaging of the rotator cuff tendon: interobserver agreement and analysis of interpretive errors. Radiology 1997;204(1):191–4.
[49] Hodler J, Kursunoglu-Brahme S, Snyder SJ, Cervilla V, Karzel RP, Schweitzer ME, et al. Rotator cuff disease: assessment with MR arthrography versus standard MR imaging in 36 patients with arthroscopic confirmation. Radiology 1992; 182(2):431–6.
[50] Flannigan B, Kursunoglu-Brahme S, Snyder S, Karzel R, Del Pizzo W, Resnick D. MR arthrography of the shoulder: comparison with conventional MR imaging. AJR Am J Roentgenol 1990; 155(4):829–32.
[51] Palmer WE, Brown JH, Rosenthal DI. Rotator cuff: evaluation with fat-suppressed MR arthrography. Radiology 1993;188(3):683–7.
[52] Ferrari FS, Governi S, Burresi F, Vigni F, Stefani P. Supraspinatus tendon tears: comparison of US and MR arthrography with surgical correlation. Eur Radiol 2002;12(5):1211–7.
[53] Meister K, Thesing J, Montgomery WJ, Indelicato PA, Walczak S, Fontenot W. MR arthrography of partial thickness tears of the undersurface of the rotator cuff: an arthroscopic correlation. Skeletal Radiol 2003;26.
[54] Yamazaki Y, Moro K. MRI by infusing xylocaine and Gd-DTPA into the subacromial bursa. J Shoulder Elbow Surg 1995;4:S87.
[55] Gartsman GM. Combined arthroscopic and open treatment of tears of the rotator cuff. J Bone Joint Surg Am 1997;79(5):776–83.
[56] Ellman H. Diagnosis and treatment of incomplete rotator cuff tears. Clin Orthop 1990; 254:64–74.
[57] McConville OR, Iannotti JP. Partial-thickness tears of the rotator cuff: evaluation and management. J Am Acad Orthop Surg 1999;7(1): 32–43.
[58] Farley TE, Neumann CH, Steinbach LS, Jahnke AJ, Petersen SS. Full-thickness tears of the rotator cuff of the shoulder: diagnosis with MR imaging. AJR Am J Roentgenol 1992; 158(2):347–51.
[59] Warner JJ, Goitz RJ, Irrgang JJ, Groff YJ. Arthroscopic-assisted rotator cuff repair: patient selection and treatment outcome. J Shoulder Elbow Surg 1997;6(5):463–72.
[60] Zanetti M, Gerber C, Hodler J. Quantitative assessment of the muscles of the rotator cuff with magnetic resonance imaging. Invest Radiol 1998 Mar;33(3):163–70.
[61] Cvitanic O, Schimandle J, Cruse A, Minter J. The acromioclavicular joint cyst: glenohumeral joint

communication revealed by MR arthrography. J Comput Assist Tomogr 1999;23(1):141–3.
[62] Sanders TG, Tirman PF, Feller JF, Genant HK. Association of intramuscular cysts of the rotator cuff with tears of the rotator cuff: magnetic resonance imaging findings and clinical significance. Arthroscopy 2000;16(3):230–5.
[63] Patten RM. Tears of the anterior portion of the rotator cuff (the subscapularis tendon): MR imaging findings. AJR Am J Roentgenol 1994; 162(2):351–4.
[64] Pfirrmann CW, Zanetti M, Weishaupt D, Gerber C, Hodler J. Subscapularis tendon tears: detection and grading at MR arthrography. Radiology 1999;213(3):709–14.
[65] Nove-Jesserand L, Gereber C, Walch G. Lesions of the anterior-superior rotator cuff. In: Warner JJP, Iannotti JP, Gerber C, editors. Complex and revision problems in shoulder surgery. Philadelphia: Lippincott-Raven; 1997. p. 165–76.
[66] Beall DP, Williamson EE, Ly JQ, Adkins MC, Emery RL, Jones TP, et al. Association of biceps tendon tears with rotator cuff abnormalities: degree of correlation with tears of the anterior and superior portions of the rotator cuff. AJR Am J Roentgenol 2003;180(3):633–9.
[67] Earwaker J. Isolated avulsion fracture of the lesser tuberosity of the humerus. Skeletal Radiol 1990;19(2):121–5.
[68] Coates MH, Breidahl W. Humeral avulsion of the anterior band of the inferior glenohumeral ligament with associated subscapularis bony avulsion in skeletally immature patients. Skeletal Radiol 2001;30(12):661–6.
[69] Bennett WF. Arthroscopic repair of isolated subscapularis tears: a prospective cohort with 2- to 4-year follow-up. Arthroscopy 2003;19(2): 131–43.
[70] Bassett RW, Cofield RH. Acute tears of the rotator cuff. The timing of surgical repair. Clin Orthop 1983;175:18–24.
[71] Zanetti M, Weishaupt D, Jost B, Gerber C, Hodler J. MR imaging for traumatic tears of the rotator cuff: high prevalence of greater tuberosity fractures and subscapularis tendon tears. AJR Am J Roentgenol 1999;172(2):463–7.
[72] Grainger AJ, Tirman PF, Elliott JM, Kingzett-Taylor A, Steinbach LS, Genant HK. MR anatomy of the subcoracoid bursa and the association of subcoracoid effusion with tears of the anterior rotator cuff and the rotator interval. AJR Am J Roentgenol 2000;174(5): 1377–80.
[73] Neer CS II. Displaced proximal humeral fractures: I. Classification and evaluation. J Bone Joint Surg Am 1970;52(6):1077–89.
[74] Mason BJ, Kier R, Bindleglass DF. Occult fractures of the greater tuberosity of the humerus: radiographic and MR imaging findings. AJR Am J Roentgenol 1999;172(2):469–73.
[75] de la Puente R, Boutin RD, Theodorou DJ, Hooper A, Schweitzer M, Resnick D. Post-traumatic and stress-induced osteolysis of the distal clavicle: MR imaging findings in 17 patients. Skeletal Radiol 1999;28(4):202–8.
[76] Demirhan M, Imhoff AB, Debski RE, Patel PR, Fu FH, Woo SL. The spinoglenoid ligament and its relationship to the suprascapular nerve. J Shoulder Elbow Surg 1998;7(3):238–43.
[77] Pasila M, Jaroma H, Kiviluoto O, Sundholm A. Early complications of primary shoulder dislocations. Acta Orthop Scand 1978;49(3):260–3.
[78] Turner JW, Parsonage MJ. Neuralgic amyotrophy (paralytic brachial neuritis); with special reference to prognosis. Lancet 1957;273(6988):209–12.
[79] Fink GR, Haupt WF. Neuralgic amyotrophy (Parsonage-Turner syndrome) following streptokinase thrombolytic therapy. [in German]. Dtsch Med Wochenschr 1995;120(27):959–92.
[80] Fleckenstein JL, Watumull D, Conner KE, Ezaki M, Greenlee RG Jr, Bryan WW, et al. Denervated human skeletal muscle: MR imaging evaluation. Radiology 1993;187(1):213–8.
[81] Bendszus M, Koltzenburg M, Wessig C, Solymosi L. Sequential MR imaging of denervated muscle: experimental study. AJNR Am J Neuroradiol 2002;23(8):1427–31.